

# The Thermal Model and the Tsallis Distribution at the Large Hadron Collider

J. Cleymans

**Abstract** An analysis is presented of identified particles at the Large Hadron Collider. Possible deviations from standard statistical distributions are investigated by considering in detail the Tsallis distribution. Matter-antimatter production is discussed within the framework of chemical equilibrium in p-p and heavy ion collisions.

## 1 The Hadronic World

The available energy for heavy ions at the Large Hadron Collider (LHC) is  $\sqrt{s} = 2760$  AGeV yet the observed temperature is only of the order of  $T \approx 0.160$  GeV. To understand this enormous change from the initial state to the final state we first clarify how this temperature is determined. There are several independent ways of doing this.

1. From the number of hadronic resonances listed in the particle data booklet [1]. This method was first proposed by Hagedorn [2]. Note that this involves no transverse momentum spectrum, no energy distribution, only the number of particles listed in the PDG [1] table. A recent updated version of this determination is shown in Fig. 1 where the logarithm of the number of resonances below a certain mass [3] is plotted versus the mass. The fitted line corresponds to a Hagedorn temperature of

$$T_H = 174 \pm 11 \text{ MeV.} \quad (1)$$

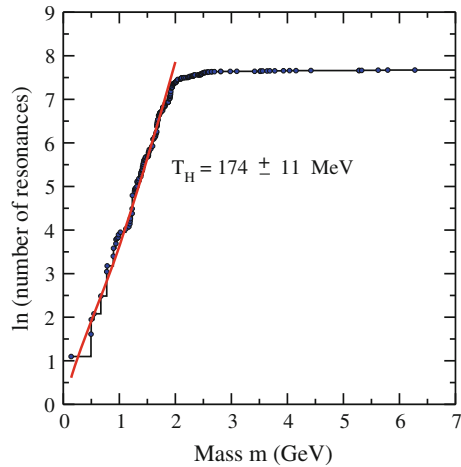
Other recent determinations are consistent with this value [4–7]. At masses above 3 GeV the increase stops due to the difficulty in identifying heavy hadronic resonances, a situation which will probably never be resolved experimentally.

---

J. Cleymans (✉)

UCT-CERN Research Centre and Department of Physics, University of Cape Town,  
Cape Town, South Africa  
e-mail: jean.cleymans@uct.ac.za

**Fig. 1** Cumulative number of hadronic resonances as a function of  $m$  [3]. The hadronic data include baryons, mesons and also heavy resonances made up of charm and *bottom* quarks



2. The multiplicity of particles in the final state. This has been an ongoing effort for the past two decades [8–10]. Again this involves no transverse momentum or energy distribution. In this case it is only the number of identified particles in the final state. The temperature at  $\mu_B = 0$  is remarkably close to the original Hagedorn temperature [2] obtained by summing the number of hadronic resonances.
3. The critical temperature determined from Lattice QCD is again remarkably close to the Hagedorn temperature and to the chemical freeze-out temperature at  $\mu_B = 0$  [11, 12].
4. The temperature can also be determined from the slope of the transverse momentum spectrum. This leads to a lower temperature, at least in p-p collisions and will be discussed below.

## 2 Transverse Momentum Distribution

The Tsallis distribution has gained prominence recently in high energy physics with high quality fits of the transverse momentum distributions made by the STAR [13] and PHENIX [14] collaborations at the Relativistic Heavy Ion Collider and by the ALICE [15], CMS [16] and ATLAS [17] collaborations at the Large Hadron Collider.

In the literature there exists more than one version of the Tsallis distribution [18, 19]. In this paper we investigate a version which we consider suited for describing results in high energy particle physics. Our main guiding criterium will be thermodynamic consistency which has not always been implemented correctly. The explicit form which we use is [20]:

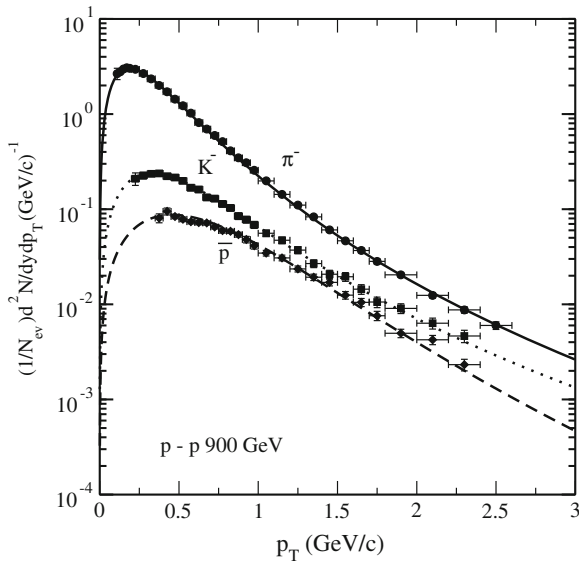


**Fig. 2** Fit to the data [15] using the Tsallis distribution [20]

$$\frac{d^2 N}{dp_T dy} = gV \frac{p_T m_T \cosh y}{(2\pi)^2} \left[ 1 + (q-1) \frac{m_T \cosh y - \mu}{T} \right]^{q/(1-q)}, \quad (2)$$

where  $p_T$  and  $m_T$  are the transverse momentum and mass respectively,  $y$  is the rapidity,  $T$  and  $\mu$  are the temperature and the chemical potential,  $V$  is the volume,  $g$  is the degeneracy factor.

The motivation for preferring this form is presented in detail in [20]. The parameterization given in Eq. (2) is close (but different) from the one used by STAR, PHENIX, ALICE, CMS and ATLAS [13–17]:

$$\frac{d^2 N}{dp_T dy} = p_T \frac{dN}{dy} \frac{(n-1)(n-2)}{nC(nC + m_0(n-2))} \left( 1 + \frac{m_T - m_0}{nC} \right)^{-n}, \quad (3)$$

where  $n$ ,  $C$  and  $m_0$  are fit parameters. The analytic expression used in Refs. [13–16] corresponds to identifying

$$n \rightarrow \frac{q}{q-1} \quad (4)$$

and

$$nC \rightarrow \frac{T + (q-1)m}{q-1}. \quad (5)$$

But differences do not allow for the above identification to be made complete due to an additional factor of the transverse mass on the right-hand side. In particular,

**Table 1** Fitted values of the  $T$  and  $q$  parameters for strange particles measured by the ALICE [15] and CMS collaborations [16] using the Tsallis-B form for the momentum distribution

Particle	$q$	$T$ (GeV)
$\pi^+$	$1.154 \pm 0.036$	$0.0682 \pm 0.0026$
$\pi^-$	$1.146 \pm 0.036$	$0.0704 \pm 0.0027$
$K^+$	$1.158 \pm 0.142$	$0.0690 \pm 0.0223$
$K^-$	$1.157 \pm 0.139$	$0.0681 \pm 0.0217$
$K_S^0$	$1.134 \pm 0.079$	$0.0923 \pm 0.0139$
$p$	$1.107 \pm 0.147$	$0.0730 \pm 0.0425$
$\bar{p}$	$1.106 \pm 0.158$	$0.0764 \pm 0.0464$
$\Lambda$	$1.114 \pm 0.047$	$0.0698 \pm 0.0148$
$\Xi^-$	$1.110 \pm 0.218$	$0.0440 \pm 0.0752$

no clear pattern emerges for the values of  $n$  and  $C$  while an interesting regularity is obtained for  $q$  and  $T$  as seen in Table 1. The striking feature is that the values of  $q$  are consistently between 1.1 and 1.2 for all species of hadrons. The fit to negatively charged particles in p-p collisions measured by the ALICE collaboration is shown in Fig. 2. An interpretation of the parameter  $q$  in terms of fluctuations around a Boltzmann distribution has been given in [21, 22].

### 3 Antimatter

One of the striking features of particle production at high energies is the near equal abundance of matter and antimatter in the central rapidity region [23, 24]. As is well known, a similar symmetry existed in the initial stage of the early universe and it still remains a mystery as to how this got lost in the subsequent evolution of the universe reaching a stage with no visible amounts of antimatter being present.

Closely related to this matter/antimatter symmetry is the production of light anti-nuclei, hypernuclei, and antihypernuclei at high energies. Since the first observation of hypernuclei in 1952 [25], there has been a steady interest in searching for new hypernuclei, exploring the hyperon-nucleon interaction which is relevant (see, e.g., [26, 27]) for nuclear physics. Hypernuclei decay with a lifetime which depends on the strength of the hyperon-nucleon interaction. While several hypernuclei have been discovered since the first observations in 1952, no antihypernucleus has ever been observed until the recent discovery of the antihypertriton in Au+Au collisions at  $\sqrt{s_{NN}} = 200$  GeV by the STAR collaboration at RHIC [28]. The yield of (anti)hypernuclei measured by STAR is very large, in particular, they seem to be produced with a similar yield as other (anti)nuclei, in particular (anti)helium-3. This abundance is much higher than measured for hypernuclei and nuclei at lower energies [29]. It is of interest to understand the nature of this enhancement, and for this the mechanism of production of (anti)hypernuclei should be investigated.

The thermalization assumption applies successfully to hadrons produced in a large number of particle and nuclear reactions at different energies (see, e.g., [30–34]). This

fact allows us to estimate thermal parameters characterizing the particle source for each colliding system, relevant for the understanding of the thermal properties of dense and hot matter, and in particular for studies of QCD phase transitions.

Using the parameterizations of thermal parameters found in the THERMUS model [35, 36], estimates have been made of the yields of (anti)hypernuclei, that can be directly compared to the recently measured yields at RHIC, as well as of (anti)matter and (anti)hypernuclei production at the Large Hadron Collider (LHC) [37]. A similar analysis, not including p-p results, has been presented recently in [38] where it was shown that ratios of hypernuclei to nuclei show an energy dependence similar to the  $K^+/\pi^+$  one with a clear maximum at lower energies.

A quantitative study as to how the matter/antimatter symmetry is reached as the beam energy is increased has been presented in [37]; estimates of ratios of hypernuclei and antihypernuclei yields in Au+Au collisions at RHIC using the above mentioned parameterizations of thermal parameters that best fit hadron production at RHIC have also been presented [37]. The analysis uses a thermal model and aims to elucidate the production mechanism of hypernuclei and antihypernuclei in heavy ion collisions at RHIC and LHC energies, thus providing insight in the surprising increase of (anti)hypernuclei production at high energies.

In heavy-ion collisions the increase in the antimatter to matter ratio with the center-of-mass energy of the system has been observed earlier by the NA49 [39, 40] and the STAR [13] collaborations. The trend of the  $\bar{p}/p$  ratio increase with the energy towards unity is shown in Fig. 3, where the open squares refer to heavy ion collisions and the solid circles refer to p-p collisions. It includes results from the NA49 [39], STAR [13] and the new results from the ALICE collaboration [24]. The two input parameters, the chemical freeze-out temperature  $T$  and the baryon chemical potential  $\mu_B$  as a function of  $\sqrt{s}$  are taken from Ref. [10]. The solid circles represent  $\mu_B$ , obtained after fitting experimental data with the THERMUS model [35, 36]. The solid line is a new parameterization adjusted for p-p collisions [37]. In view of the fact that peripheral and central collisions show no noticeable change in the temperature, the same  $T$  dependence for p-p as in heavy ion collisions was used [37]. It is important to note that  $\mu_B$  is always lower in p-p collisions than in heavy ion collisions, e.g., the freeze-out chemical potential follows a different pattern, due to the lower stopping power in p-p collisions.

The relation between the  $\bar{p}/p$  ratio and  $\mu_B$  can be shown easily within the statistical concept using the Boltzmann statistics. The production of light nuclei including hypertritons ( ${}^3_{\Lambda}\text{H}$ ) and antihypertritons ( ${}^3_{\Lambda}\bar{\text{H}}$ ) was recently observed by the STAR collaboration [28]. The abundances of such light nuclei and antinuclei follow a consistent pattern in the thermal model. The temperature remains the same as before but an extra factor of  $\mu_B$  is picked up each time the baryon number is increased. Each proton or neutron thus simply adds a factor of  $\mu_B$  to the Boltzmann factor. The production of nuclear fragments is therefore very sensitive to the precise value of the baryon chemical potential and could thus lead to a precise determination of  $\mu_B$ . Deuterium has an additional neutron and the antideuterium to deuterium ratio is given by the square of the antiproton to proton ratio:

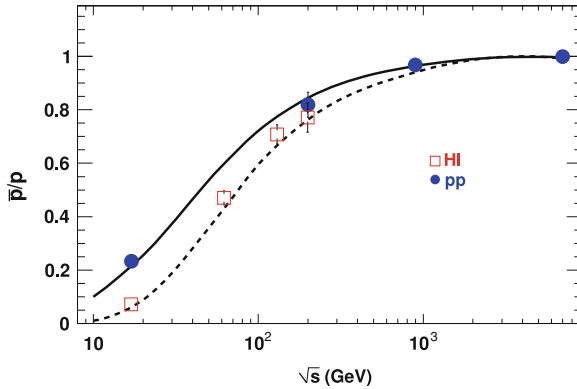


**Fig. 3** The  $\bar{p}/p$  ratio as function of  $\sqrt{s}$ . The *solid circles* are results from p-p collisions and the *open squares* are results from HI collisions as a function of the invariant beam energy [13, 23, 24, 39, 40]

$$\frac{n_{\bar{d}}}{n_d} = e^{-(4\mu_B)/T}. \quad (6)$$

Helium-3 has three nucleons and the corresponding antihelium-3 to helium-3 ratio is given by

$$\frac{n_{3\bar{\text{He}}}}{n_{3\text{He}}} = e^{-(6\mu_B)/T}. \quad (7)$$

If the nucleus carries strangeness, this leads to an extra factor of  $\mu_S$

$$\frac{n_{\Lambda^3\bar{\text{H}}}}{n_{\Lambda^3\text{H}}} = e^{-(6\mu_B - 2\mu_S)/T}. \quad (8)$$

In mixed ratios, the different degeneracy factors are also taken into account, e.g., 6 for  ${}^3_{\Lambda}H$  and 2 for  ${}^3_{\Lambda}H$

$$\frac{n_{\Lambda^3\text{H}}}{n_{3\text{He}}} = 3e^{-(6\mu_B - \mu_S)/T}. \quad (9)$$

A detailed description of the results can be found in [37, 38, 41].

## 4 Conclusions

The Tsallis distribution gives a very good description of the transverse momentum spectrum, the parameter  $q$  which is a measure for the deviation from a standard Boltzmann distribution is found to be around 1.1. The thermal model provides valuable insights in the composition of the final state produced in heavy ion and in

p-p collisions. It shows a clear systematic way of interpreting results concerning identified particles. The production of antimatter like antinuclei, hypernuclei and antihypernuclei shows a new region of applications for the thermal model which promises to be very useful.

**Acknowledgments** Numerous discussions with S. Kabana, A. Kalweit, I. Kraus, K. Redlich, H. Oeschler, N. Sharma, A. Sorin and D. Worku are at the basis of the results presented here.

## References

1. C. Caso et al. (Particle Data Group), *Eur. Phys. J.* **3**, 1 (2008)
2. R. Hagedorn, *Supp. Nuovo Cimento* **III**, 147 (1965)
3. J. Cleymans, D. Worku, *Mod. Phys. Lett. A* **26**, 1197 (2011)
4. S. Chatterjee, S. Gupta, R.M. Godbole, *Phys. Rev. C* **81**, 044907 (2010)
5. W. Broniowski, W. Florkowski, *Phys. Lett. B* **490**, 223 (2000)
6. W. Broniowski, contribution to the Proceedings of the Mini-Workshop “Few-Quark Problems”, Bled, Slovenia, 8–15 July 2000, arXiv:hep-ph/0008112
7. W. Broniowski, W. Florkowski, L.Y. Glozman, *Phys. Rev. D* **70**, 117503 (2004)
8. A. Andronic, P. Braun-Munzinger, J. Stachel, *Nucl. Phys. A* **834**, 237C (2010)
9. F. Becattini, J. Manninen, M. Gazdzicki, *Phys. Rev. C* **73**, 044905 (2006)
10. J. Cleymans, H. Oeschler, K. Redlich, S. Wheaton, *Phys. Rev. C* **73**, 034905 (2006)
11. S. Borsanyi et al. (Wuppertal-Budapest Collaboration), *JHEP* **1009**, 073 (2010)
12. M. Cheng, S. Ejiri, P. Hegde, F. Karsch, O. Kaczmarek, E. Laermann, R.D. Mawhinney, C. Miao et al., *Phys. Rev. D* **81**, 054504 (2010)
13. B.I. Abelev et al. (STAR), *Phys. Rev. C* **75**, 064901 (2007)
14. A. Adare et al. (PHENIX), *Phys. Rev. C* **83**, 064903 (2011)
15. K. Aamodt et al. (ALICE Collaboration), *Eur. Phys. J. C* **71**, 1655 (2011)
16. V. Khachatryan et al. (CMS), *JHEP* **05**, 064 (2011)
17. G. Aad et al. (ATLAS Collaboration), *New J. Phys.* **13**, 053033 (2011)
18. C. Tsallis, *J. Stat. Phys.* **52**, 479 (1988)
19. C. Tsallis, R.S. Mendes, A.R. Plastino, *Phys. A* **261**, 534 (1998)
20. J. Cleymans, D. Worku, *J. Phys. G* **39**, 025006 (2012)
21. G. Wilk, Z. Włodarczyk, *Phys. Rev. Lett.* **84**, 2770 (2000)
22. G. Wilk, Z. Włodarczyk, *Eur. Phys. J. A* **40**, 299 (2009)
23. B.I. Abelev et al. (STAR Collaboration), *Phys. Rev. C* **79**, 034909 (2009)
24. K. Aamodt et al. (ALICE Collaboration), *Phys. Rev. Lett.* **106**, 072002 (2010)
25. M. Danysz, J. Pniewski, *Phil. Mag.* **44**, 348 (1953)
26. D. Hahn, H. Stöcker, *Nucl. Phys. A* **476** (1988)
27. H. Stöcker, W. Greiner, *Phys. Rep.* **137**, 277 (1986)
28. B.I. Abelev et al. (STAR Collaboration), *Science* **328**, 58 (2010)
29. R. Rapp, E.V. Shuryak, *Phys. Rev. Lett.* **86**, 2980 (2001)
30. F. Becattini, *Z. Phys. C* **76**, 269 (1997)
31. F. Becattini, U. Heinz, *Z. Phys. C* **69**, 485 (1996)
32. K. Redlich, J. Cleymans, H. Oeschler, A. Tounsi, *Acta Phys. Pol. B* **33**, 1609 (2002)
33. P. Braun-Munzinger, K. Redlich, J. Stachel, *nucl-th/0304013*, *Invited Review in Quark Gluon Plasma 3*, ed. by R.C. Hwa, X.N. Wang, (World Scientific Publishing, 2004)
34. P. Braun-Munzinger, J. Cleymans, H. Oeschler, K. Redlich, *Nucl. Phys. A* **697**, 902 (2002)
35. S. Wheaton, J. Cleymans, *J. Phys. G* **31**, S1069 (2005)

36. S. Wheaton, J. Cleymans, M. Hauer, *Comput. Phys. Commn.* **180**, 84 (2009)
37. J. Cleymans, S. Kabana, I. Kraus, H. Oeschler, K. Redlich, N. Sharma, *Phys. Rev. C* **84**, 054916 (2011)
38. A. Andronic, P. Braun-Munzinger, J. Stachel, H. Stöcker, S., *Phys. Lett. B* **697**, 203 (2011)
39. C. Alt et al. (NA49 Collaboration), *Phys. Rev. C* **73**, 044910 (2005)
40. C. Alt et al. (NA49 Collaboration), *Phys. Rev. C* **77**, 024903 (2008)
41. A. Andronic, P. Braun-Munzinger, J. Stachel, *Nucl. Phys. A* **772**, 167 (2006)